

## Evidence for Bardeen-Cooper-Schrieffer-type superconducting behavior in the electride $(\text{CaO})_{12}(\text{Al}_2\text{O}_3)_7:e^-$ from heat capacity measurements

Yoshimitsu Kohama,<sup>1</sup> Sung Wng Kim,<sup>2</sup> Takeo Tojo,<sup>1</sup> Hitoshi Kawaji,<sup>1</sup> Tooru Atake,<sup>1</sup> Satoru Matsuishi,<sup>2</sup> and Hideo Hosono<sup>1,2</sup>

<sup>1</sup>*Materials and Structures Laboratory, Tokyo Institute of Technology, Mail-Box R3-7, 4259 Nagatsuta-cho, Midori-ku, Yokohama 226-8503, Japan*

<sup>2</sup>*Frontier Collaborative Research Center, Tokyo Institute of Technology, Mail-Box S2-13, 4259 Nagatsuta-cho, Midori-ku, Yokohama 226-8503, Japan*

(Received 10 October 2007; revised manuscript received 20 January 2008; published 12 March 2008)

The heat capacity of the single crystalline electride of  $(\text{CaO})_{12}(\text{Al}_2\text{O}_3)_7:e^-$  (C12A7: $e^-$ ) with  $T_c=0.2$  K was larger than that of electron-undoped C12A7 in the temperature range 0.085–5 K, reflecting the metallic nature of the electride. A superconducting transition was detected as a heat capacity jump  $\Delta C_p=3.4$  mJ mol<sup>-1</sup> K<sup>-1</sup>, and the profile and magnitude of  $\Delta C_p$  agreed well with those expected from the BCS theory. The electron-phonon coupling constant ( $\lambda\sim 0.46$ ) and Debye temperature ( $\Theta_D\sim 630$  K) were much larger than those for alkali metals having  $s$ -like conduction electrons as in the present electride, suggesting that electrides having a rigid structure will be a class of BCS superconductors.

DOI: 10.1103/PhysRevB.77.092505

PACS number(s): 74.25.Bt, 74.25.Jb, 75.40.Cx

Electrides are a family of ionic crystals in which electrons serve as anions.<sup>1</sup> These electrides have attracted much attention from material scientists because of their exotic nature and expectation for unique properties. The main drawbacks delaying investigations into the properties and applications of these materials concern the thermal and chemical instabilities. This obstacle was resolved by utilizing an inorganic nanoporous crystal,  $(\text{CaO})_{12}(\text{Al}_2\text{O}_3)_7$  (C12A7), as the complex forming material for electrons instead of organic compounds.<sup>2</sup> We previously explored the functionalities of C12A7 electrides (C12A7: $e^-$ ) and reported that they exhibit metal-insulator transitions<sup>3</sup> and have a very low intrinsic work function (2.4 eV) comparable to potassium metal, irrespective of being chemically inert in an ambient atmosphere.<sup>4</sup> Recently, a superconducting transition was found at 0.2–0.4 K for C12A7: $e^-$  doped with anionic electrons to  $2\times 10^{21}$  cm<sup>-3</sup>.<sup>5</sup> The anionic electrons, which are loosely accommodated in the subnanometer-sized cages of C12A7, are in an  $s$ -like state in the ground state, as clarified in the previous papers.<sup>6,7</sup> Thus, the electronic state of C12A7: $e^-$  is similar to that of  $s$ -band metals such as alkali metals. It is a well-known fact that  $s$ -band metals do not show a superconducting transition at an ambient pressure.<sup>8–10</sup> In this Brief Report, we examine the mechanism of the superconducting transition in C12A7: $e^-$  by measuring the low temperature heat capacity and clarifying the difference between C12A7: $e^-$  and alkali metals (as a typical  $s$ -band metal) in terms of physical parameters extracted from the analysis of low temperature heat capacity data.

First, the unique features of C12A7: $e^-$  are explained on the basis of crystal structure. C12A7 is a nanoporous crystal with cubic symmetry (lattice constant=1.199 nm) and has two chemical formulas in the unit cell.<sup>11,12</sup> This lattice framework having a chemical formula  $[\text{Ca}_{24}\text{Al}_{28}\text{O}_{64}]^{4+}$  consists of 12 subnanometer-sized cages. Each cage has an inner diameter of  $\sim 0.4$  nm and is connected to eight neighboring cages via open mouths with a monomolecular layer thick wall to form a three-dimensional structure [Fig. 1(a)]. The extra-framework  $\text{O}^{2-}$  ions (“free oxygen ions”) occupy 2 of the 12

cages to maintain charge neutrality, and the chemical formula of the C12A7 unit cell is thus represented as  $[\text{Ca}_{24}\text{Al}_{28}\text{O}_{64}]^{4+}(2\text{O}^{2-})$ . The free oxygen ions can be replaced by other anions such as  $\text{F}^-$ ,<sup>13</sup>  $\text{Cl}^-$ ,<sup>13</sup>  $\text{OH}^-$ ,<sup>14</sup> and even electrons ( $e^-$ ).<sup>2</sup> The electride C12A7: $e^-$  is obtained by substituting the free oxygen ion with two electrons, and the unit cell is described as  $[\text{Ca}_{24}\text{Al}_{28}\text{O}_{64}]^{4+}(4e^-)$ . Calculations based on an embedded-cluster model,<sup>6</sup> and experimental approaches employing photoemission spectroscopy,<sup>4</sup> revealed that the three-dimensional connection of the empty cages gives rise to an additional conduction band named the “cage conduction band (CCB).” This CCB is located  $\sim 2$  eV below the bottom of the “framework conduction band,” as shown in Fig. 1(b),<sup>3,4,7</sup> and is partially occupied by the anionic electrons having an  $s$ -like nature, as shown in Fig. 1(a).<sup>6,7</sup> Therefore, the  $s$ -like CCB plays a decisive role in the metallic behavior and superconductivity of C12A7: $e^-$ .<sup>3,4,7</sup> Since such an  $s$ -like band is unfavorable for the emergence of superconductivity as evidenced by the cases of alkali metals, it is interesting to investigate the mechanism for the superconductivity in C12A7: $e^-$  in comparison with alkali metals. In this work, we measured the heat capacity and magnetic field dependence for C12A7: $e^-$  single crystals. The superconducting phase transition was detected as a heat capacity jump in a single crystalline C12A7: $e^-$  sample with the highest concentration of anionic electrons, and the mechanism of the superconductivity was discussed on the basis of the results obtained.

The single crystals of C12A7 were grown by the floating-zone (FZ) method<sup>15</sup> or by the Czochralski (CZ) method.<sup>16</sup> The FZ single crystals were transparent and colorless, while the CZ single crystals were transparent with a slight orange coloration due to a trace impurity ( $\sim 5\times 10^{17}$  cm<sup>-3</sup>) of  $\text{Ir}^{4+}$  ions which were unintentionally incorporated from an Ir crucible used in the CZ process. A specimen obtained by heating an FZ-grown single crystal, C12A7, with Ti metal at 1100 °C for 24 h in an evacuated silica tube is named as sample A, and that obtained by heating a CZ-grown crystal is named as sample B. The concentrations of anionic electrons

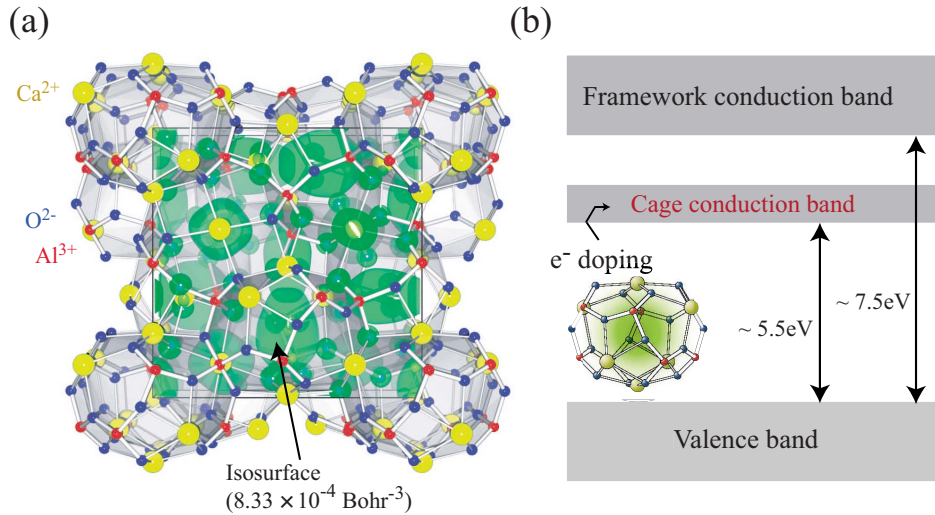


FIG. 1. (Color online) (a) Crystal structure overlapped with the isosurface of the electron density occupying the cage conduction band (CCB). Red, yellow, and blue spheres represent Al, Ca, and O atoms, respectively. The gray frame indicates the cubic unit cell containing twelve cages, and the lattice constant (cubic symmetry) is  $\sim 1.2$  nm. One of the cages has a free space with an inner diameter of  $\sim 0.4$  nm. The isosurface, colored light green, was obtained by *ab initio* density functional theory calculations using the VASP code (Ref. 33). The Fermi level is located in CCB and is primarily composed of *s*-like electrons trapped in the empty cage. (b) Electronic structure. There are two types of conduction bands. One conduction band is constituted of a cage framework and another (CCB) is composed of three-dimensionally connected empty cages. The band gap between the valence band and framework conduction band is  $\sim 7.5$  eV, and the cage conduction band is located  $\sim 2$  eV below the framework conduction band (Ref. 4).

in samples A and B were evaluated as  $\sim 2 \times 10^{21} \text{ cm}^{-3}$  from optical reflectance measurements.<sup>17</sup> Sample C was obtained by heating an FZ single crystal sample at  $700^\circ \text{C}$  for 5 days in the presence of calcium metal in a silica glass tube, and the anionic electron concentration was estimated as  $\sim 8 \times 10^{20} \text{ cm}^{-3}$ .<sup>17</sup> Superconductivity was found only for sample A from electrical resistance and magnetic susceptibility measurements down to  $0.085 \text{ K}$ .<sup>5</sup>

The heat capacity of the samples was measured with a homemade relaxation-type calorimeter using a  $^3\text{He}/^4\text{He}$  dilution refrigerator in the temperature range  $0.085\text{--}5 \text{ K}$ . The amounts of samples used for the heat capacity measurements were  $60\text{--}90 \text{ mg}$ . The experimental apparatus and procedure used were the same as those used for the previous heat capacity measurements performed on the mother compound, C12A7.<sup>18</sup>

The inset of Fig. 2 shows the  $C_p T^{-1}$  versus  $T^2$  plot of the three samples A, B, and C together with the data of C12A7.<sup>18</sup> Each of the three samples having anionic electrons has a larger heat capacity than the electron-undoped C12A7 sample in the whole temperature region. The plots of data on the three samples apparently lie on the straight lines, indicating that the heat capacity can be fitted to a well-known equation  $C_p = \beta T^3 + \gamma T$  like a normal metal. The  $\beta T^3$  term denotes the lattice contribution and  $\gamma T$  is the electronic heat capacity that is observed in systems with itinerant electrons. If the anionic electrons are localized as  $F^+$ -like centers in C12A7:  $e^-$ , the  $T$ -linear term ( $\gamma T$ ) should not be observed in  $C_p$  in this temperature range. Therefore, the present results substantiate the delocalized nature of anionic electrons in C12A7:  $e^-$ . On the other hand, the data of C12A7 do not fit with a straight line passing through the origin. The nonzero

intercept for the electron-undoped C12A7 is attributed to the disordered nature of a free oxygen ion in the cage, as reported previously.<sup>18</sup>

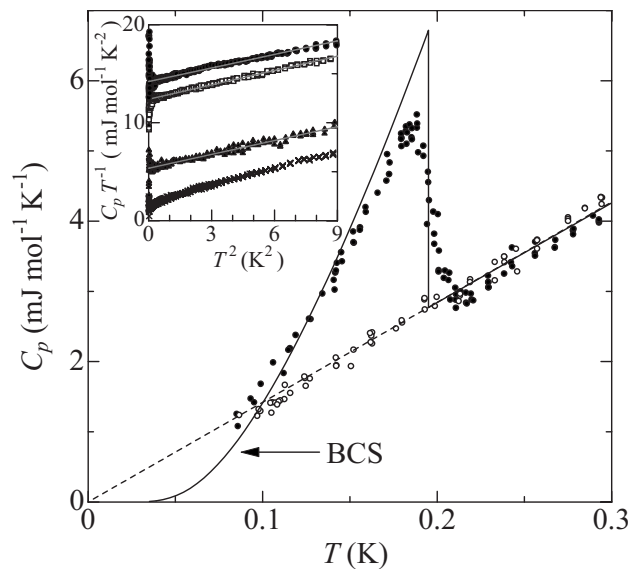


FIG. 2. Heat capacities of sample A under zero magnetic field (solid circles) and under the magnetic field of  $0.1 \text{ T}$  (open circles). The broken line is given by  $C_p = \beta T^3 + \gamma T$ , as discussed in the text. The solid curve is the theoretical curve associated with the BCS theory, as reported in Ref. 24. The inset shows  $C_p$  versus  $T^2$  plots of samples A (solid circles), B (open squares), C (solid triangles), and C12A7 (crosses, Ref. 18). The lines were obtained by least squares fitting of the data between  $0.3$  and  $3 \text{ K}$  to  $C_p = \beta T^3 + \gamma T$ .

The parameters for each sample are determined from the slopes and intercepts in the inset of Fig. 2:  $\beta = 0.46 \pm 0.02 \text{ mJ mol}^{-1} \text{ K}^{-4}$ ,  $\gamma = 14.2 \pm 0.3 \text{ mJ mol}^{-1} \text{ K}^{-2}$  for sample A,  $\beta = 0.49 \pm 0.02 \text{ mJ mol}^{-1} \text{ K}^{-4}$ ,  $\gamma = 12.4 \pm 0.3 \text{ mJ mol}^{-1} \text{ K}^{-2}$  for sample B, and  $\beta = 0.47 \pm 0.02 \text{ mJ mol}^{-1} \text{ K}^{-4}$ ,  $\gamma = 5.4 \pm 0.3 \text{ mJ mol}^{-1} \text{ K}^{-2}$  for sample C. It is worth noting that sample A showing superconductivity has the highest value of  $\gamma$  among the three samples. In degenerate semiconductors, the value of  $\gamma$  increases monotonically with the increase of electron concentration.<sup>19</sup> Therefore, it is consistent with the fact that sample A has the highest concentration of anionic electrons. The coefficient  $\gamma$  is directly related to the density of states at the Fermi level,  $N_\gamma(0)$ ,

$$\gamma = \frac{1}{3} \pi^2 k_B^2 N_\gamma(0), \quad (1)$$

where  $k_B$  is the Boltzmann constant. The values of  $N_\gamma(0)$  are obtained as  $(7.0 \pm 0.1) \times 10^{21}$ ,  $(6.1 \pm 0.1) \times 10^{21}$ , and  $(2.6 \pm 0.1) \times 10^{21} \text{ eV}^{-1} \text{ cm}^{-3}$  for samples A, B, and C, respectively. These values are  $\sim 1/2$  to  $1/5$  of alkali metals [Li:  $32.5 \times 10^{21} \text{ eV}^{-1} \text{ cm}^{-3}$  (Ref. 20); Na:  $15.5 \times 10^{21} \text{ eV}^{-1} \text{ cm}^{-3}$  (Ref. 21); K:  $12.4 \times 10^{21} \text{ eV}^{-1} \text{ cm}^{-3}$  (Ref. 22); Rb:  $11.7 \times 10^{21} \text{ eV}^{-1} \text{ cm}^{-3}$  (Ref. 22)].

The coefficient  $\beta$  represents the lattice contribution relating to the Debye temperature  $\Theta_D$  and is given by

$$\Theta_D = \left( \frac{12\pi^4 Rr}{5\beta} \right)^{1/3}, \quad (2)$$

where  $r$  is the number of atoms in the chemical formula and  $R$  is the gas constant. The  $\Theta_D$  of samples A, B, and C are calculated as  $628 \pm 9$ ,  $616 \pm 9$ , and  $622 \pm 9 \text{ K}$ , respectively. It is interesting to note that the  $\Theta_D$  of C12A7: $e^-$  is very close to that ( $604 \text{ K}$ ) of electron-undoped C12A7,<sup>18</sup> which is quite different from the case of conventional semiconductors. For example, for heavily boron-doped diamond exhibiting a superconducting transition, the  $\Theta_D$  is lower by 23% than that of undoped diamond.<sup>23</sup> The conventional carrier doping in semiconductors is attained by the atomic replacement with impurity in the rigid lattice framework. Consequently, the high density carrier doping leads to a weakening of the bonds constituting the rigid lattice framework and thus the decrease of  $\Theta_D$ . On the other hand, the carrier doping of C12A7: $e^-$  is attained by the exchange of the extra-framework oxygen ions accommodated in the cage with anionic electrons. Therefore, the carrier doping does not affect the rigid lattice framework, and thus the value of  $\Theta_D$  remains unchanged.

The main panel of Fig. 2 shows the low temperature heat capacity of sample A under magnetic fields of  $H=0 \text{ T}$  and  $H=0.1 \text{ T}$ . The superconducting transition temperature  $T_c$  defined as the midpoint of the jump was  $0.195 \pm 0.02 \text{ K}$  and the jump disappeared under a magnetic field of  $0.1 \text{ T}$ . Both of these results agree well with those of the previous report.<sup>5</sup> The height of the heat capacity jump at  $T_c$ ,  $\Delta C_p$ , was  $3.4 \text{ mJ mol}^{-1} \text{ K}^{-1}$ , and the normalized value of  $\Delta C_p / \gamma T_c$  was 1.22. In the present system, the heat capacity peak is somewhat broadened due presumably to the residual free oxygen ions, which give rise to the slight decrease of  $\Delta C_p / \gamma T_c$ . Tak-

ing into account this decrease, we may conclude that the value of  $\Delta C_p / \gamma T_c$  agrees with the well-known value in the weak-coupling BCS prediction ( $\Delta C_p / \gamma T_c = 1.43$ ). In addition, the temperature profile of the jump in  $C_p$  is in good agreement with that derived from the weak-coupling BCS theory, as shown in Fig. 2.<sup>24</sup> On the basis of these agreements, we conclude that the superconductivity of C12A7: $e^-$  is categorized into a weak-coupling BCS superconductor.

In BCS superconductors, once  $\Theta_D$  and  $T_c$  are known, one may estimate the electron-phonon coupling constant  $\lambda$ , following McMillan's formula,<sup>25</sup>

$$T_c = \left( \frac{\Theta_D}{1.45} \right) \exp \left[ - \frac{1.04(1+\lambda)}{\lambda - \mu^*(1+0.62\lambda)} \right], \quad (3)$$

where  $\mu^*$  is the Coulomb pseudopotential. Assuming a value of  $\mu^* = 0.20 \pm 0.05$ , which is reported in the low density systems (Li metal,<sup>26</sup> Si clathrate compound,<sup>27,28</sup> alkali-metal-doped fullerene,<sup>29</sup> and so on), the value of  $\lambda = 0.46 \pm 0.08$  is obtained from the experimental evaluated values of  $\Theta_D = 628 \pm 9 \text{ K}$  and  $T_c = 0.195 \text{ K}$ . The magnitude of  $\lambda$ , which is in the weak-coupling regime, is in agreement with the analysis of  $\Delta C_p$ , as described above. In Eq. (3), the superconducting transition temperature  $T_c$  increases with increasing  $\lambda$ .  $\lambda$  is expressed by  $\lambda = N_\gamma(0)V$ , where  $V$  is the pairing interaction, and  $N_\gamma(0)$  directly affects the value of  $T_c$ . In the present study, the superconducting transition was observed in only sample A with the highest  $N_\gamma(0)$  among the three samples. In addition, the increase in anionic electron concentration leads to an increase of  $T_c$  in the C12A7: $e^-$  film samples via an increase in  $N_\gamma(0)$ .<sup>5</sup> Therefore, the variation of  $T_c$  in C12A7: $e^-$  with respect to the carrier concentration may be explained by Eq. (3).

Finally, we would like to consider how the crystal structure affects the emergence of a superconducting transition in comparison with alkali metals. Like alkali metals, the Fermi level located in the conduction band (CCB) of C12A7: $e^-$  is composed of  $s$  electrons.<sup>7</sup> It is well known that the experimental absence of a superconducting transition for alkali metals at ambient pressure is understandable within the framework of the BCS theory.<sup>8-10</sup> Electron-phonon interactions [Li,  $\lambda = 0.38$  (Ref. 30); Na,  $\lambda = 0.20$  (Ref. 31); K,  $\lambda = 0.14$  (Ref. 31); Rb,  $\lambda = 0.14$  (Ref. 31)] and values of  $\Theta_D$  [Li,  $\Theta_D = 420 \text{ K}$  (Ref. 32); Na,  $\Theta_D = 150 \text{ K}$  (Ref. 32); K,  $\Theta_D = 100 \text{ K}$  (Ref. 32)] are rather smaller than those ( $\lambda = 0.46$ ,  $\Theta_D = 628 \text{ K}$ ) of C12A7: $e^-$ . The high value of  $\Theta_D$  is due to the rigid lattice framework of C12A7: $e^-$ , which is primarily composed of strong bonding between the tetrahedral  $\text{Al}^{3+}$  and oxygen ions. On the other hand, the relatively high  $\lambda$  for C12A7: $e^-$  may be responsible for the three-dimensionally connected subnanometer-sized cages which work as electron pathways. This implies that the itinerant electrons primarily populated in the nanospace are favorable over the case that electrons are populated in the  $s$  orbitals of constituting atoms. Following this simple guideline, we may expect that electrides with a rigid framework structure will be a class of BCS superconductors.

In summary, we measured the heat capacity of the electride C12A7: $e^-$  with various anionic electron concentrations

of  $(0.8-2) \times 10^{21} \text{ cm}^{-3}$  in the temperature range 0.085–5 K. The  $T$ -linear term ( $\gamma T$ ) in the heat capacity originating from the metallic nature of the electrider was observed. In the sample having the highest density of state (sample A), the superconducting transition was observed as a heat capacity jump  $\Delta C_p = 3.4 \text{ mJ mol}^{-1} \text{ K}^{-1}$  at  $T_c = 0.195 \text{ K}$ , which disappeared in the presence of a weak magnetic field of 0.1 T. The height of the heat capacity jump and the temperature dependence of heat capacity below  $T_c$  revealed that the superconductivity of C12A7: $e^-$  is categorized into a weak-coupling

BCS type. The C12A7 electrider is discriminated from alkali metals with respect to the strong electron-phonon interaction and high Debye temperature.

This work was supported by a Grant-in-Aid for Creative Scientific Research (No. 16GS0205) from the Ministry of Education, Culture, Sports, Science and Technology of the Japanese Government and the Asahi Glass Foundation, Japan.

- 
- <sup>1</sup>J. L. Dye, *Inorg. Chem.* **36**, 3816 (1997).  
<sup>2</sup>S. Matsuishi, Y. Toda, M. Miyakawa, K. Hayashi, T. Kamiya, M. Hirano, I. Tanaka, and H. Hosono, *Science* **301**, 626 (2003).  
<sup>3</sup>S. W. Kim, S. Matsuishi, T. Nomura, Y. Kubota, M. Takata, K. Hayashi, T. Kamiya, M. Hirano, and H. Hosono, *Nano Lett.* **7**, 1138 (2007).  
<sup>4</sup>Y. Toda, H. Yanagi, E. Ikenaga, J. J. Kim, M. Kobata, S. Ueda, T. Kamiya, M. Hirano, K. Kobayashi, and H. Hosono, *Adv. Mater. (Weinheim, Ger.)* **19**, 3564 (2007).  
<sup>5</sup>M. Miyakawa, S. W. Kim, M. Hirano, Y. Kohama, H. Kawaji, T. Atake, H. Ikegami, K. Kono, and H. Hosono, *J. Am. Chem. Soc.* **129**, 7270 (2007).  
<sup>6</sup>P. V. Sushko, A. L. Shluger, K. Hayashi, M. Hirano, and H. Hosono, *Phys. Rev. Lett.* **91**, 126401 (2003).  
<sup>7</sup>P. V. Sushko, A. L. Shluger, M. Hirano, and H. Hosono, *J. Am. Chem. Soc.* **129**, 942 (2007).  
<sup>8</sup>The  $s$ -band metals such as alkali metals are known to be unfavorable for superconductivity. Only Li metal shows a superconductivity with very low transition temperature ( $T_c = 0.4 \text{ mK}$ ) at ambient pressure (Ref. 9).  
<sup>9</sup>J. Tuoriniemi, K. Juntunen-Nurmilaukas, J. Uusvuori, E. Pentti, A. Salmela, and A. Sebedash, *Nature (London)* **447**, 187 (2007).  
<sup>10</sup>D. A. Papaconstantopoulos, L. L. Boyer, B. M. Klein, A. R. Williams, V. L. Moruzzi, and J. F. Janak, *Phys. Rev. B* **15**, 4221 (1977).  
<sup>11</sup>H. Bartl and T. Scheller, *Neues Jahrb. Mineral., Monatsh.* **35**, 547 (1970).  
<sup>12</sup>H. Hosono and Y. Abe, *Inorg. Chem.* **26**, 1192 (1987).  
<sup>13</sup>J. Jeevaratnam, F. P. Glasser, and L. S. D. Glasser, *J. Am. Ceram. Soc.* **47**, 105 (1964).  
<sup>14</sup>J. A. Imlach, L. S. D. Glasser, and F. P. Glasser, *Cem. Concr. Res.* **1**, 57 (1971).  
<sup>15</sup>S. Watauch, I. Tanaka, K. Hayashi, M. Hirano, and H. Hosono, *J. Cryst. Growth* **237-239**, 801 (2002).  
<sup>16</sup>K. Kurashige, Y. Toda, S. Matsuishi, K. Hayashi, M. Hirano, and H. Hosono, *Cryst. Growth Des.* **6**, 1602 (2006).  
<sup>17</sup>S. Matsuishi, S. W. Kim, T. Kamiya, M. Hirano, and H. Hosono, *J. Phys. Chem. C* (to be published).  
<sup>18</sup>Y. Kohama, T. Tojo, H. Kawaji, T. Atake, S. Matsuishi, and H. Hosono, *Chem. Phys. Lett.* **421**, 558 (2006).  
<sup>19</sup>Y. Matsushita, P. A. Wiannecki, A. T. Sommer, T. H. Geballe, and I. R. Fisher, *Phys. Rev. B* **74**, 134512 (2006).  
<sup>20</sup>D. L. Martin, *Proc. R. Soc. London, Ser. A* **263**, 378 (1961).  
<sup>21</sup>C. S. Barrett, *Acta Crystallogr.* **9**, 671 (1956).  
<sup>22</sup>W. H. Lien and N. E. Phillips, *Phys. Rev.* **133**, A1370 (1964).  
<sup>23</sup>V. A. Sidorov, E. A. Ekimov, E. D. Bauer, N. N. Mel'nik, N. J. Curro, V. Fritsch, J. D. Thompson, S. M. Stishov, A. E. Alexenko, and B. V. Spitsyn, *Diamond Relat. Mater.* **14**, 335 (2005).  
<sup>24</sup>B. Mühlischlegel, *Z. Phys.* **155**, 313 (1959).  
<sup>25</sup>W. L. McMillan, *Phys. Rev.* **167**, 331 (1968).  
<sup>26</sup>C. F. Richardson and N. W. Ashcroft, *Phys. Rev. B* **55**, 15130 (1997).  
<sup>27</sup>K. Tanigaki, T. Shimizu, K. M. Itoh, J. Teraoka, Y. Moritomo, and S. Yamanaka, *Nat. Mater.* **2**, 653 (2003).  
<sup>28</sup>D. Connétable, V. Timoshevskii, B. Masenelli, J. Beille, J. Marcus, B. Barbara, A. M. Saitta, G. M. Rignanese, P. Melinon, S. Yamanaka, and X. Blase, *Phys. Rev. Lett.* **91**, 247001 (2003).  
<sup>29</sup>O. Gunnarsson, *Rev. Mod. Phys.* **69**, 575 (1997).  
<sup>30</sup>G. Profeta, C. Franchini, N. N. Lathiotakis, A. Floris, A. Sanna, M. A. L. Marques, M. Lüders, S. Massidda, E. K. U. Gross, and A. Continenza, *Phys. Rev. Lett.* **96**, 047003 (2006).  
<sup>31</sup>A. H. MacDonald and C. R. Leavens, *Phys. Rev. B* **26**, 4293 (1982).  
<sup>32</sup>E. S. R. Gopal, *Specific Heats at Low Temperatures* (Heywood Books, London, 1966).  
<sup>33</sup>G. Kresse and J. Furthmüller, *Phys. Rev. B* **54**, 11169 (1996).